The Journal of Experimental Biology 207, 993-1004
Published by The Company of Biologists 2004
doi:10.1242/jeb.00850

Allometry of kinematics and energetics in carpenter bees (*Xylocopa varipuncta*) hovering in variable-density gases

Stephen P. Roberts[1,*], Jon F. Harrison[2] and Robert Dudley[3,4]

[1]*Department of Biological Sciences, University of Nevada, Las Vegas, 4505 S. Maryland Parkway, Las Vegas, NV 89154-4004, USA*, [2]*School of Life Sciences, Arizona State University, Tempe, AZ 85287-1501, USA*, [3]*Department of Integrative Biology, University of California, Berkeley, CA 94720-3140, USA* and [4]*Smithsonian Tropical Research Institute, PO Box 2072, Balboa, Republic of Panama*

*Author for correspondence (e-mail: sroberts@ccmail.nevada.edu)

Accepted 28 December 2003

Summary

We assessed the energetic and aerodynamic limits of hovering flight in the carpenter bee *Xylocopa varipuncta*. Using normoxic, variable-density mixtures of O_2, N_2 and He, we were able to elicit maximal hovering performance and aerodynamic failure in the majority of bees sampled. Bees were not isometric regarding thorax mass and wing area, both of which were disproportionately lower in heavier individuals. The minimal gas density necessary for hovering (*MGD*) increased with body mass and decreased with relative thoracic muscle mass. Only the four bees in our sample with the highest body mass-specific thorax masses were able to hover in pure heliox. Wingbeat frequency and stroke amplitude during maximal hovering were significantly greater than in normodense hovering, increased significantly with body mass during normodense hovering but were mass independent during maximal hovering. Reserve capacity for wingbeat frequency and stroke amplitude decreased significantly with increasing body mass, although reserve capacity in stroke amplitude (10–30%) exceeded that of wingbeat frequency (0–8%). Stroke plane angle during normodense hovering was significantly greater than during maximal hovering, whereas body angle was significantly greater during maximal hovering than during normodense hovering. Power production during normodense hovering was significantly less than during maximal hovering. Metabolic rates were significantly greater during maximal hovering than during normodense hovering and were inversely related to body mass during maximal and normodense hovering. Metabolic reserve capacity averaged 34% and was independent of body mass. Muscle efficiencies were slightly higher during normodense hovering. The allometry of power production, power reserve capacity and muscle efficiency were dependent on the assumed coefficient of drag (C_D), with significant allometries most often at lower values of C_D. Larger bees operate near the envelope of maximal performance even in normodense hovering due to smaller body mass-specific flight muscles and limited reserve capacities for kinematics and power production.

Key words: aerodynamics, allometry, energetics, flight, reserve capacity, *Xylocopa*, bee.

Introduction

Hovering insects attain mass-specific rates of metabolism and mechanical power production that are among the highest recorded in the animal kingdom. Even so, rapid vertical ascent and the ability to lift substantial loads are common features of natural flight behavior in many insects, indicating the presence of considerable lift and power reserves relative to normal hovering. Biomechanical underpinnings to such aerodynamic and energetic capacity have been assessed primarily through the use of tethering and by mass-loading *via* food ingestion or the addition of artificial weights. Nectar loading in freely hovering honeybees (*Apis mellifera*; Wolf et al., 1989) and bumblebees (*Bombus* spp.; Heinrich, 1975) increases metabolic expenditures up to 44% and 100%, respectively, above unloaded hovering values, but neither maximal performance nor mechanical power output were investigated in these studies. *Drosophila* increase vertical flight forces by up to 70% and metabolic rates up to 27% during the transition from tethered flight, in which lift equals body mass, to maximal flight force production (Lehmann and Dickinson, 1998; Lehmann et al., 2000). During free flight, weight attachments can increase flight forces of *Drosophila* by approximately 100% (Lehmann and Dickinson, 1997; Lehmann, 1999; see also Marden, 1987).

The use of tethering and attachment of weights potentially influence both the behavioral motivation to fly and features of flight capacity (Dudley and Chai, 1996; Willmott and Ellington, 1997; Dudley, 2000). For example, weight addition may significantly alter the insect's center of gravity (although cumulatively applied loading to dragonflies suggests no effect on capacity; Marden, 1987) whereas tethering may artificially

constrain body orientation to non-preferred angles. Some of these issues can be circumvented by use of normoxic but hypodense gas mixtures to elicit increases in lift and power. Orchid bees (*Eulaema* sp. and *Euglossa* spp.) are capable of hovering in normoxic heliox (density of 0.41 kg m^{-3}) and increase power production by ~45% relative to flight in normal air (Dudley, 1995). By contrast, ruby-throated hummingbirds (*Archilocus colubris*; mass of 3–4 g) hovering in normoxic helium/nitrogen mixtures exhibit aerodynamic failure at densities intermediate to those of normodense air and heliox (0.50–0.79 kg m^{-3}, depending on lipid loading and molt condition; Chai and Dudley, 1995, 1996, 1999; Chai et al., 1996; Chai, 1997). In this group, metabolic and aerodynamic power reserves relative to hovering in normal conditions average 36% and 25%, respectively. Both orchid bees and hummingbirds increase stroke amplitude in response to hypodense challenge, although complementary changes in angle of attack and wing rotation speed at the ends of half-strokes await testing *via* high-speed video analysis. The general nature of modulatory responses to flight in hypodense air is not clear, however, given that only two volant taxa have been studied to date.

Here, we examine the hovering flight of carpenter bees (*Xylocopa varipuncta*) in variable-density but normoxic gas mixtures (Dudley and Chai, 1996) to assess aerodynamic and metabolic limits to flight performance. We chose *Xylocopa* to assess maximal hovering performance because their basic flight physiology is well understood (Chappell, 1982; Nicolson and Louw, 1982; Heinrich and Buchmann, 1986; King et al., 1996; Gäde de and Auerswald, 1998) and because these bees are more heavily wing loaded than orchid bees (Nicolson and Louw, 1982; Casey et al., 1985; Dudley, 1995). Hovering capacity in hypodense air is inversely proportional to wing loading (e.g. Chai et al., 1996), and *Xylocopa* is thus more likely than orchid bees to fail at low gas densities that are experimentally feasible. Carpenter bees also exhibit a wide range of body masses intraspecifically, which enables allometric analysis of limits to flight performance without untoward complications of phylogenetic variance. Also, changes in metabolism and kinematics in low-density, high-thermal conductance gas mixtures should, in *Xylocopa*, reflect aerodynamic responses as opposed to thermoregulatory responses. The latter might be expected by species, such as honeybees (Harrison et al., 1996; Roberts and Harrison, 1999) and various *Centris* spp (Spangler and Buchmann, 1991; Roberts et al., 1998), that thermoregulate during hovering flight by varying kinematics and metabolic heat production. However, because *Xylocopa* hovering flight metabolism is independent of air temperature between 22°C and 38°C (Chappell, 1982; Nicolson and Louw, 1982), increases in *Xylocopa* metabolism/kinematic performance in hypodense gases should not be confounded by an aerodynamically mediated thermoregulatory response as described above. Finally, oxygen diffusivity is inversely proportional to gas density, and thus tracheal diffusion is substantially enhanced in O_2/N_2/He mixtures. It is extremely unlikely that O_2 diffusion would limit kinematic and metabolic performance during flight in hypodense gas mixtures (Dudley and Chai, 1996). Flight of *Xylocopa* in variable-density gases thus offers an excellent opportunity to assess the allometry, kinematics and energetics of maximal hovering flight performance.

Materials and methods

Flight kinematics and morphological variables

Individual *Xylocopa varipuncta* Patton females were netted as they flew in the Life Science Courtyard of Arizona State University, Tempe, AZ, USA. Immediately after capture, individuals were transferred to the laboratory and were placed in a 30 cm×30 cm×30 cm lucite flight chamber fitted at opposite ends with eight evenly spaced inlet and outlet ports for gas perfusion. A 2 cm-wide layer of packed glass wool was positioned in the chamber just downstream from the inlet ports to provide even airflow through the flight chamber, which was housed in an environmental room maintained at 25±0.5°C. Wingbeat kinematics of hovering bees were obtained using the protocols of Dudley (1995). Briefly, a video camera (Panasonic AG456) positioned above the chamber recorded horizontal projections of wingbeat kinematics, whereas lateral views of the hovering insect were simultaneously filmed from reflections in a mirror positioned at 45° to one face of the chamber. Wingbeat frequencies were recorded acoustically with a microphone located within the flight chamber; microphone output was recorded on the audio track of the videotape.

Each bee was exposed, in random but non-repeating order, to six variable-density gas mixtures ranging in density from 0.41 kg m^{-3} to 1.21 kg m^{-3} (Table 1), the latter value corresponding to normodense air. Canisters of pure O_2, N_2 and He were used with calibrated flow rotameters to generate experimental gas mixtures and subsequently to flush the flight chamber at a rate of 60 l min^{-1} (STP). This gas infusion yielded an approximate mean flow velocity of 0.01 m s^{-1} through the chamber. Individual bees were flown within each gas mixture for 3 min. If bees landed, they were immediately persuaded to fly or attempt flight by chasing them with a small magnet on the bottom of the chamber that could be moved using a magnetic wand moved around the external surface of the chamber floor. Bees that landed on the sides of the chamber

Table 1. *Variable-density gas mixtures presented in random order to* Xylocopa varipuncta *females*

Gas mixture	% O_2	% N_2	% He	Density (kg m^{-3})
1	21	79.0	0.0	1.21
2	21	63.2	15.8	1.04
3	21	47.4	31.6	0.88
4	21	31.6	47.4	0.72
5	21	15.8	63.2	0.57
6	21	0.0	79.0	0.41

were immediately persuaded to fly or attempt flight by tapping on the external surface of the chamber. The kinematic analysis was limited to data from flight bouts within the last 2 min of exposure to both normal air and the minimal gas density necessary for hovering. Aerodynamic failure was defined as the inability of an individual to ascend two or more body lengths from the chamber floor and then hover for at least 2 s. Dynamic viscosities of gas mixtures were calculated using the formulae of Reid et al. (1987).

Wingbeat kinematic parameters were determined from frame-by-frame video playbacks using a Panasonic AG1980 video player and NIH Image software and included the stroke amplitude (Φ), stroke plane angle (β) relative to the horizontal, and body angle (χ) relative to the horizontal (definitions follow Ellington, 1984c). Acoustic recordings of wingbeat frequency (f) were analyzed using SoundEdit software for Macintosh (see Roberts et al., 1998). Within each gas mixture, mean values of kinematic variables were determined from three separate measurements. Each estimate of wingbeat frequency was determined from a sequence containing 10–20 clearly distinguishable, uninterrupted wingbeats, for which the mean wingbeat frequency was determined by dividing the number of wingbeats in the sequence by the sequence duration. Only those sequences in which the insect exhibited controlled, unaccelerated flight two or more body lengths (or at least 60 mm) above the floor and away from the walls and ceiling of the flight chamber were used for analysis, so as to minimize the possibility of underestimating power due to the boundary effect – when vortices become 'trapped' between the flyer and nearby surfaces (Raynor and Thomas, 1991). Ascending, descending or maneuvering flight was ignored.

Morphological parameters for use in aerodynamic calculations were determined for each insect (Ellington, 1984b) and included body mass (M_b), relative wing mass (M_w) for both wing pairs (expressed as a fraction of body mass), wing length (R), total wing area (S; the area of both wing pairs), body length, thoracic mass and thoracic muscle mass. Thoracic muscle mass was determined indirectly by cutting the thorax (shorn of legs) in half and removing trace non-muscular features such as fats and components of the digestive tract. The two thoracic halves were weighed and then soaked in 0.5 mol l^{-1} NaOH for 24 h. The cuticular residue was weighed after digestion of the muscle tissue. Relative thoracic muscle mass (M_{muscle}) was expressed as a fraction of total body mass. Wing loading ($p_w=M_b\boldsymbol{g}/S$, where $\boldsymbol{g}$ is gravitational acceleration) and wing aspect ratio ($AR=4R^2/S$) were calculated for each bee. Non-dimensional radii for moments of wing mass, virtual mass and wing area were determined following standard methods (see Ellington, 1984b).

Lift and power requirements

Lift and power output during normal and maximal hovering flight were calculated using the aforementioned kinematic and morphological data and the aerodynamic model of Ellington (1984a–f). Mean lift coefficients (C_L) were calculated according to Ellington (1984f) such that vertical force production averaged over the wingbeat period equaled body weight. Mechanical power requirements were estimated by evaluating individual components of profile (P_{pro}) and induced (P_{ind}) power requirements. Taxa with asynchronous flight muscle, such as bees, are likely to store kinetic energy elastically during the deceleration phase of the wing stroke, so that inertial power requirements are probably negligible (see Ellington, 1984f; Dickinson and Lighton, 1995). Therefore, total power output (P_{mech}) for a flight sequence was calculated for the cases of perfect elastic storage of wing inertial energy and corresponds to the aerodynamic power requirements alone ($=P_{pro}+P_{ind}$; see Ellington, 1984f). Recent studies (Dickinson et al., 1999; Sane and Dickinson, 2001; Usherwood and Ellington, 2002) have experimentally measured unsteady drag coefficients (C_D) and demonstrate unequivocally that flow separation and leading edge vortices yield much higher drag than previously realized. Usherwood and Ellington (2002) studied continuously revolving bumblebee wing planforms at Reynolds numbers similar to those of hovering *Xylocopa* and showed that Reynolds number and aspect ratio, together with wing shape, yield small effects on drag relative to changes in the angle of attack. We did not use high-speed photography in the present study and thus were unable to measure angle of attack or its variation with air density (although this is probably a major factor during hovering in hypodense gas). Mean C_Ls for *Xylocopa* were 1.4–1.7. For bumblebee wing planforms, this range of C_Ls corresponds to the beginning of the plateau for the lift:drag polar, at which point the C_D is ~1. Sane and Dickinson (2001) demonstrate that the stroke pattern of model *Drosophila* wings that optimizes lift (where mean $C_L=1.9$) generates a mean C_D of 2.7. The Reynolds numbers are much higher in *Xylocopa*, so lift:drag ratios would in principle be higher in these large insects. Furthermore, angle of attack almost certainly changes as air density is reduced, rendering direct comparisons of calculations with a constant C_D difficult to interpret. Despite these uncertainties, we have calculated power assuming C_Ds of 1 and 3 instead of $(7/Re)^{0.5}$, where Re is the mean Reynolds number of the wing chord (see Ellington, 1984f).

Metabolic power input (P_{input}; W kg^{-1}) during hovering was estimated from measurements of rates of carbon dioxide production, which were determined using flow-through respirometry. Metabolic rates were analyzed only for periods identified on the videotape as being periods of active hovering. The gas excurrent from the flight chamber was subsampled and directed to a Licor 6252 carbon dioxide analyzer (Licor, Lincoln, NE, USA) calibrated with a known span gas and CO_2-free air. The output of the carbon dioxide analyzer was digitized and monitored online using a Sable Systems (Henderson, NV, USA) data acquisition system. Metabolic power input was calculated assuming metabolism of simple carbohydrates and a respiratory quotient of one (21.4 J ml^{-1} CO_2; Gäde de and Auerswald, 1998). Reserve capacities for kinematic parameters, mechanical power input and metabolic power output were calculated as the ratio of the difference between maximal and normodense values to the

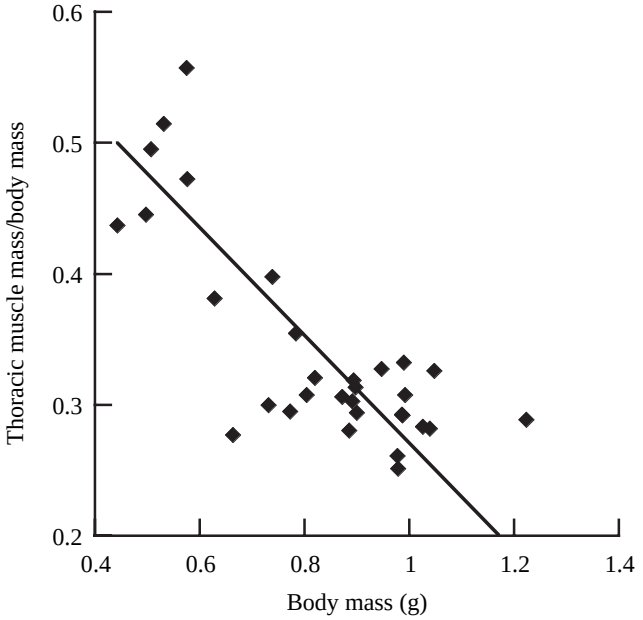

Fig. 1. Relative thoracic muscle mass (M_{muscle}) *vs* body mass (M_b) for female *Xylocopa varipuncta*. Model II regression: M_{muscle}=0.682–0.411M_b, r_{29}=–0.78, P<0.001.

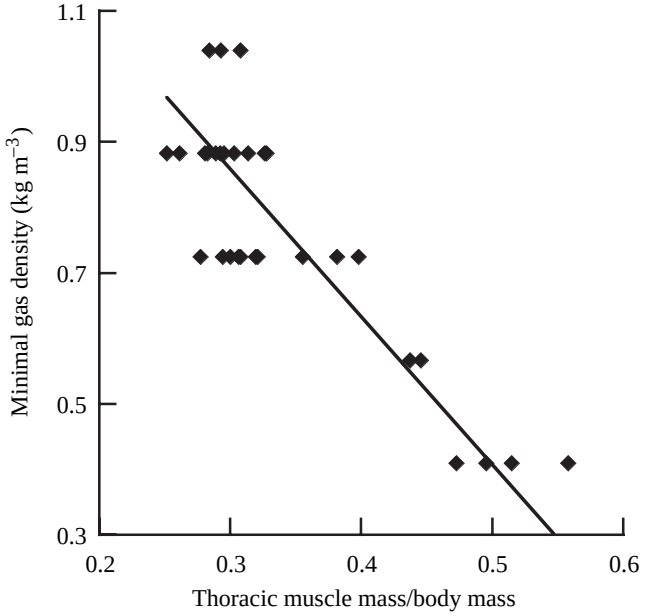

Fig. 2. Minimal gas density (*MGD*) necessary for hovering flight *vs* relative thoracic muscle mass for female *Xylocopa varipuncta*. Model II regression: *MGD*=1.536–2.256M_{muscle}, r_{28}=–0.86, P<0.001.

normodense value and were expressed as percentages. Values of muscle efficiency were calculated as the ratio of mechanical power output to metabolic power input and were also expressed as percentages.

Thoracic temperatures

We measured thoracic temperatures of all bees within 10 s of exposure to the final gas mixture used in each trial. The lid of the flight chamber was removed, the bee was gently restrained, and a microprobe thermocouple (diameter 0.33 mm; time constant 0.025 s) connected to a Physitemp BAT-12 thermometer (Clifton, NJ, USA) was inserted dorsally into the thorax.

Results

Morphological parameters

Body mass of *X. varipuncta* females was 0.838±0.194 g (mean ± S.D., N=34) and ranged from 0.443 g to 1.223 g. Abdominal mass scaled with body mass to the power of 1.69 [model II regression, log (abdominal mass)=–0.356+1.693(log M_b), r_{31}=0.95, P<0.001], whereas thoracic mass scaled with body mass to the power of 0.629 [model II regression, log (thoracic mass)=–0.436+0.629(log M_b), r_{31}=0.76, P<0.001]. Wing loading was 32.39±5.97 N m^{-2} and scaled with body mass to the power of 0.79 [model II regression, log p_w=1.579+0.818(log M_b), r_{31}=0.96, P<0.001]. Relative thoracic muscle mass averaged 0.342±0.080 (N=31) and decreased significantly with increasing body mass (Fig. 1).

Kinematics and flight performance

The minimal gas density necessary for hovering (*MGD*) was 0.771±0.187 kg m^{-3} (mean ± S.D., N=31), was positively correlated with body mass (model II regression, *MGD*=–0.001+0.928M_b, r_{29}=0.80, P<0.001) but was negatively correlated with relative thoracic muscle mass

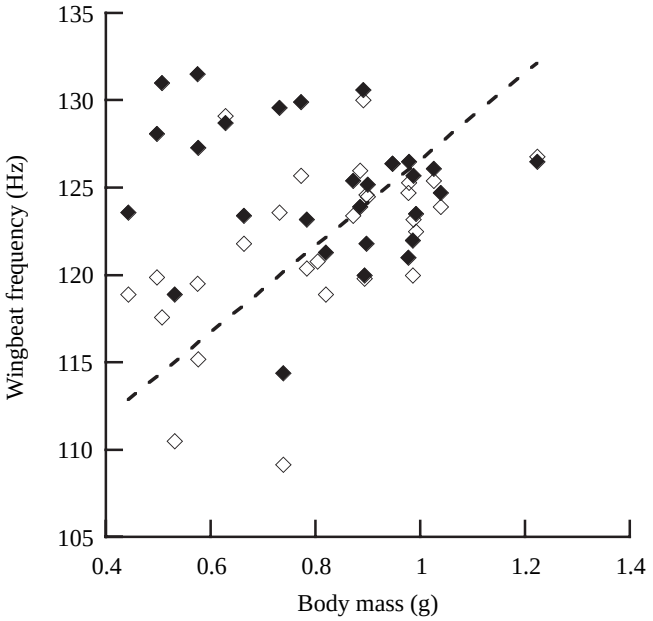

Fig. 3. Wingbeat frequency during hovering in normodense air (f_{norm}; open symbols) and during maximal hovering in hypodense air (f_{max}; filled symbols) *vs* body mass (M_b) for *Xylocopa varipuncta* females. Model II regression: f_{norm}=101.92+24.70M_b, r_{27}=0.53, P<0.005 (broken line); f_{max}=141.33–20.09M_b, r_{26}=–0.15, P=0.44.

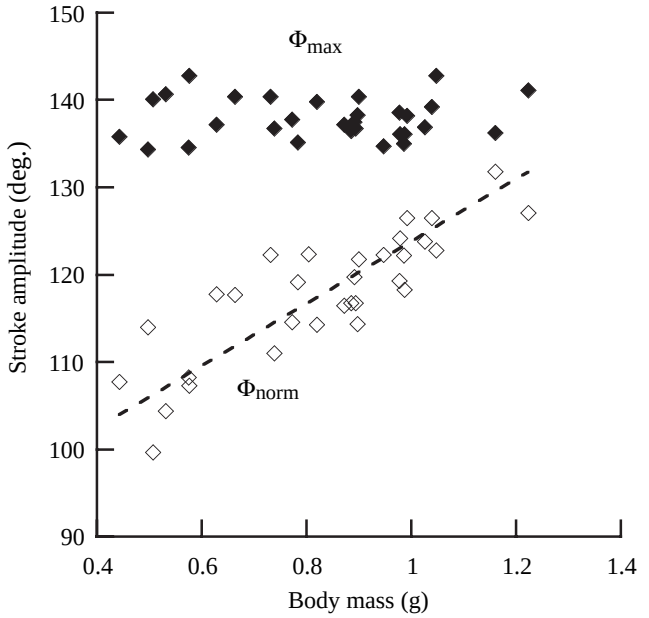

Fig. 4. Stroke amplitude during normal hovering (Φ_{norm}; open symbols) and maximal hovering (Φ_{max}; filled symbols) *vs* body mass (M_b) for *Xylocopa varipuncta* females. Model II regression: Φ_{norm}=88.22+35.58M_b, r_{29}=0.84, P<0.001 (broken line); Φ_{max}=128.26+11.62M_b, r_{28}=0.03, P=0.89.

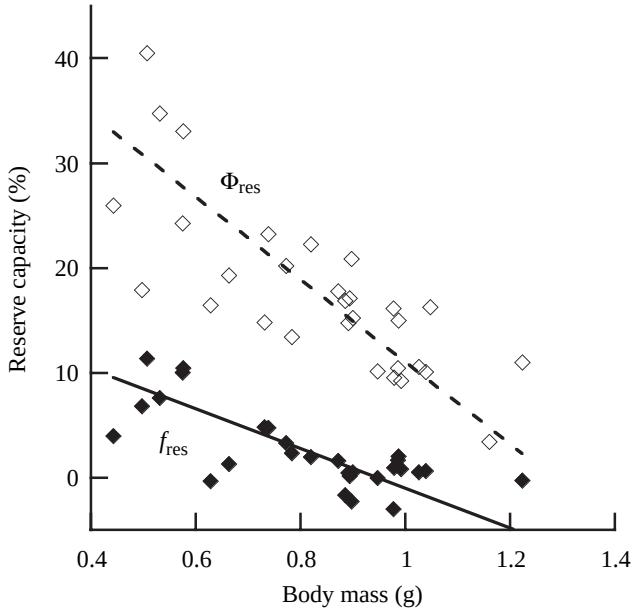

Fig. 5. Reserve capacity in wingbeat frequency (f_{res}; filled symbols) and in stroke amplitude (Φ_{res}; open symbols) *vs* body mass (M_b) for hovering *Xylocopa varipuncta* females. Model II regression: f_{res}=17.93–18.94M_b, r_{26}=–0.73, P<0.001 (solid line); Φ_{res}=50.44–39.35M_b, r_{28}=–0.78, P<0.001 (broken line).

(Fig. 2). The four bees with the highest relative thoracic muscle mass were able to fly in pure heliox (density 0.41 kg m^{-3}). For these bees, we assumed that the kinematic and energetic parameters of these individuals during hovering in heliox represented maximal performance. Wingbeat frequency during maximal hovering was 125.0±4.0 Hz (N=28) and was significantly greater (paired t-test, P=0.0013) than that in normodense hovering (122.0±4.8 Hz, N=29). Wingbeat frequency increased significantly with body mass in normodense hovering but was mass independent in maximal flight (Fig. 3). Stroke amplitude during maximal hovering was 137.9±2.4° (N=30) and was significantly greater (paired t-test, P<0.0001) than in normodense hovering (117.8±7.1°; N=31). Stroke amplitude increased significantly with body mass in normodense hovering but was mass independent during maximal hovering flight (Fig. 4). Reserve capacities for wingbeat frequency and stroke amplitude significantly decreased with increasing body mass, although reserve capacity in stroke amplitude exceeded that of wingbeat frequency across all body masses (Fig. 5).

Stroke plane angle during normodense hovering averaged 6.6±1.9° (mean ± S.D., N=31) and was significantly greater (paired t-test, P<0.0001) than that in maximal hovering (1.8±2.1°, N=30). Stroke plane angle decreased significantly with body mass in normodense hovering but was mass independent in maximal flight (Fig. 6). Body angle during maximal hovering flight was 49.2±4.2° (N=30) and was significantly greater (paired t-test, P<0.0001) than that in normodense flight (41.8±5.6°, N=31). Body angle was

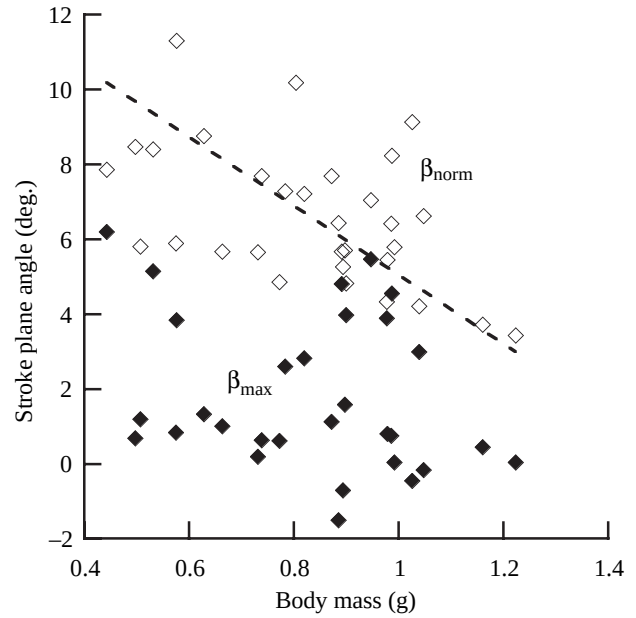

Fig. 6. Stroke plane angle during normal (β_{norm}; open symbols) and maximal hovering (β_{max}; filled symbols) *vs* body mass (M_b) for *Xylocopa varipuncta* females. Model II regression: β_{norm}=14.28–9.23M_b, r_{29}=–0.49, P<0.005 (broken line); β_{max}=10.16–10.01M_b, r_{28}=–0.26, P=0.17.

independent of body mass during both normodense (model II regression, r_{29}=0.31, P=0.08) and maximal hovering flight (model II regression, r_{28}=0.13, P=0.43). The angle of the

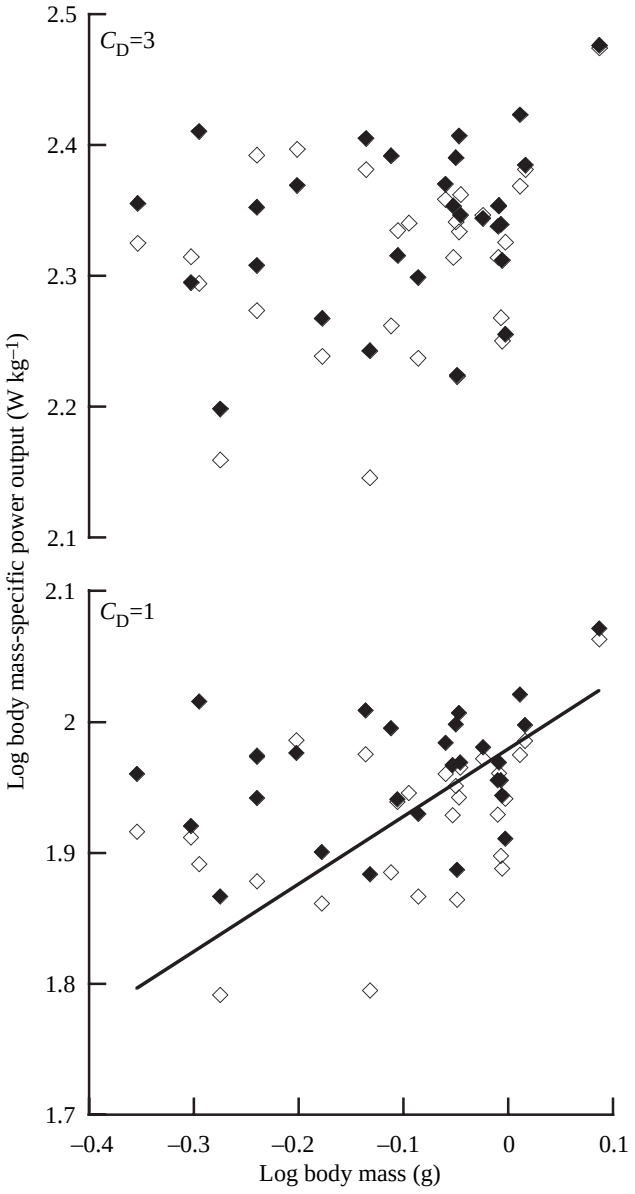

Fig. 7. Log body mass (M_b)-specific power output during normal ($P_{body,norm}$; open symbols) and maximal hovering flight ($P_{body,max}$; filled symbols) *vs* log M_b for *Xylocopa varipuncta* females. Assumed drag coefficient (C_D)=1 (bottom panel) and 3 (top panel). Model II regression for C_D=1: log $P_{body,norm}$=1.979+0.516(log M_b), r_{27}=0.43, P<0.02 (solid line); log $P_{body,max}$=2.004+0.405(log M_b), r_{26}=0.32, P=0.11. Model II regression for C_D=3: log $P_{body,norm}$=2.380+0.633(log M_b), r_{27}=0.29, P=0.13; log $P_{body,max}$=2.662+3.890(log M_b), r_{26}=0.02, P=0.89.

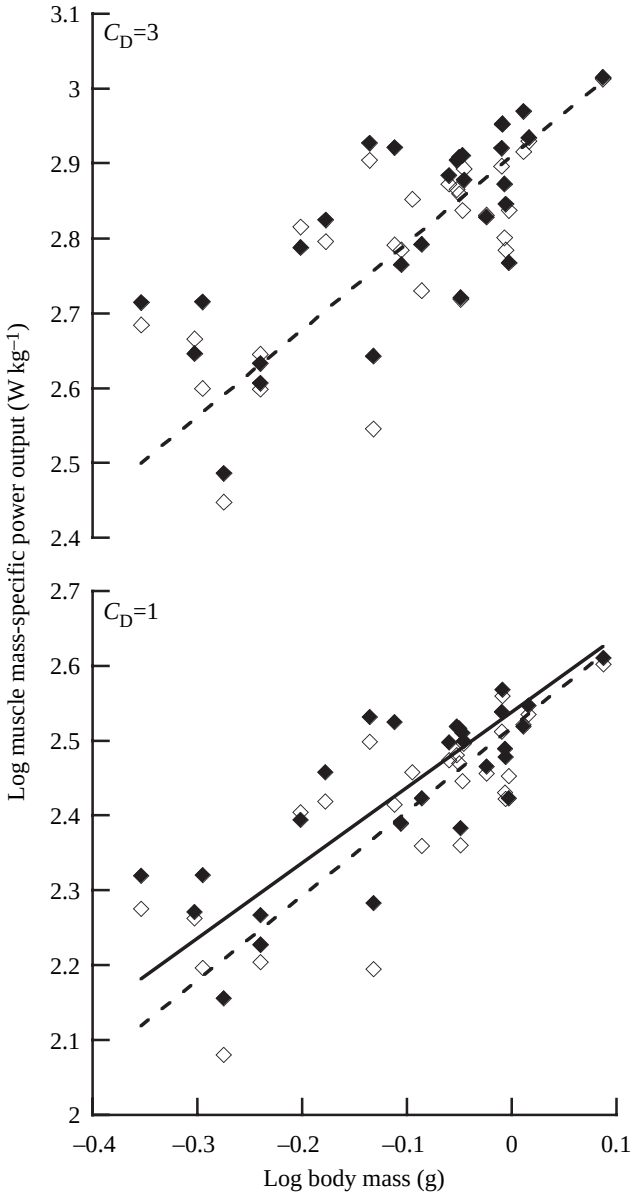

Fig. 8. Log muscle mass-specific power output during normal ($P_{muscle,norm}$; open symbols) and maximal hovering flight ($P_{muscle,max}$; filled symbols) *vs* log body mass (M_b) for *Xylocopa varipuncta* females. Assumed drag coefficient (C_D)=1 (bottom panel) and 3 (top panel). Model II regression for C_D=1: log $P_{muscle,norm}$=2.517+1.126(log M_b), r_{27}=0.82, P<0.001 (broken line); log $P_{muscle,max}$=2.538+1.007(log M_b), r_{26}=0.81, P<0.001 (solid line). Model II regression for C_D=3: log $P_{muscle,norm}$=2.909+1.160(log M_b), r_{27}=0.76, P<0.001 (broken line); log $P_{muscle,max}$=3.210+4.762(log M_b), r_{26}=0.17, P=0.38.

stroke plane relative to the body increased slightly but significantly from 48.3±4.5° during normodense hovering to 50.9±4.6° during maximal hovering (paired *t*-test, P<0.0001).

Mechanical power production

Body mass-specific power output during maximal hovering flight ($P_{body,max}$) was 92.1±9.9 W kg^{-1} and 221.3±31.9 W kg^{-1} (mean ± S.D., N=28), assuming C_Ds of 1 and 3, respectively. For both C_D values, $P_{body,max}$ was significantly greater (paired *t*-test, P<0.003) than body mass-specific power output during normal hovering flight ($P_{body,norm}$; C_D=1, 85.0±11.2 W kg^{-1}; C_D=3, 208.9±33.4 W kg^{-1}; N=29). Log $P_{body,max}$ was independent of log M_b for both C_D values, while log $P_{body,norm}$ increased significantly with log M_b assuming C_D=1 but was independent of log M_b assuming C_D=3 (Fig. 7). Muscle mass-

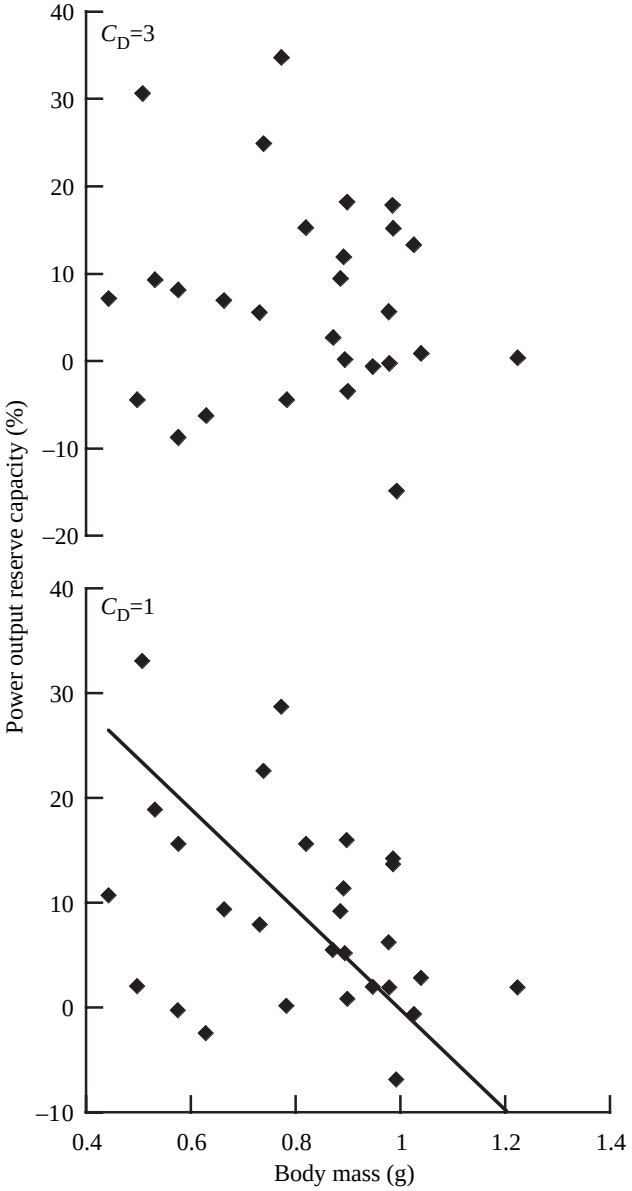

Fig. 9. Reserve capacity (%) in muscle mass-specific power output (P_{res}) *vs* body mass (M_b) for hovering *Xylocopa varipuncta* females. Assumed drag coefficient (C_D)=1 (bottom panel) and 3 (top panel). Model II regression for C_D=1: P_{res}=47.70–47.85M_b, r_{26}=–0.37, P=0.05 (solid line). Model II regression for C_D=3: P_{res}=54.74–59.05M_b, r_{26}=–0.11, P=0.59.

specific power output during maximal hovering flight ($P_{muscle,max}$) was 280.2±68.0 W kg^{-1} and 677.6±183.4 W kg^{-1} (N=28), assuming C_Ds of 1 and 3, respectively. For both C_D values, $P_{muscle,max}$ was significantly greater (paired t-test, P<0.002) than during normodense hovering ($P_{muscle,norm}$; C_D=1, 261.2±68.6 W kg^{-1}; C_D=3, 640.7±175.0 W kg^{-1}; N=29). Log $P_{muscle,max}$ significantly increased with log M_b for both C_D values, while log $P_{muscle,norm}$ significantly increased with log M_b for C_D=1 but was independent of log M_b for C_D=3 (Fig. 8). Reserve capacity for P_{muscle} significantly decreased

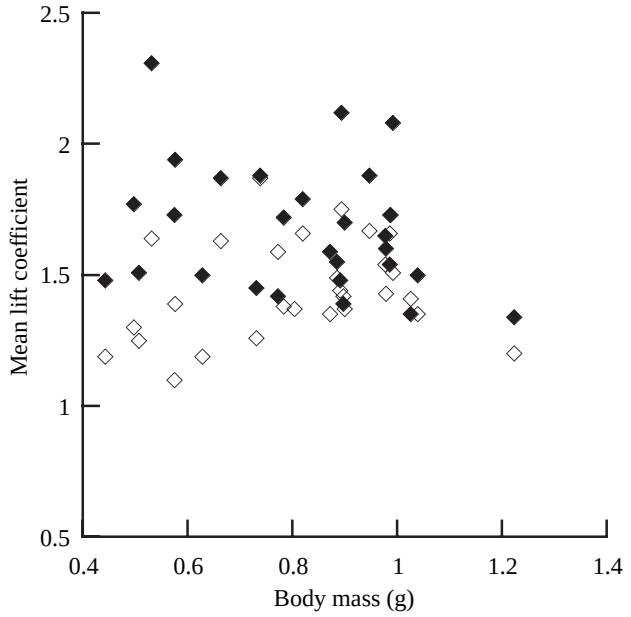

Fig. 10. Mean lift coefficient during normal ($C_{L,norm}$; open symbols) and maximal ($C_{L,max}$; filled symbols) hovering flight *vs* body mass (M_b) for *Xylocopa varipuncta* females. Model II regression: $C_{L,norm}$=0.645+0.994M_b, r_{27}=0.25, P=0.20; $C_{L,max}$=2.678–1.236M_b, r_{26}=–0.26, P=0.18.

with M_b for C_D=1 but was independent of M_b for C_D=3 (Fig. 9). The mean C_L during maximal hovering was 1.67±0.24 (N=28) and was significantly greater (paired t-test, P<0.0001) than in normodense hovering (1.45±0.19; N=29). In both cases, mean C_Ls were independent of M_b (Fig. 10).

Metabolic power requirements and body temperatures

Metabolic rate increased ~1.5-fold with decreasing air density (Fig. 11). Body mass-specific metabolic rate during maximal hovering in hypodense gases averaged 519±187 W kg^{-1} (mean ± S.D., N=24) and was significantly greater (paired t-test, P=0.0005) than during normodense hovering (393±112 W kg^{-1}, N=24; Fig. 12). Log M_b-specific metabolic rates significantly decreased with log M_b during both normal and maximal hovering flight (Fig. 12). Reserve capacity in M_b-specific metabolic power averaged 33.6±26.5% (N=24) and was independent of M_b (model II regression, r_{22}=–0.37, P=0.13). Muscle mass-specific metabolic rate during maximal hovering averaged 1491±416 W kg^{-1} (mean ± S.E.M., N=24) and was significantly greater (paired t-test, P=0.0003) than in normodense hovering (1141±243 W kg^{-1}; N=24). Neither normodense nor maximal muscle mass-specific metabolic rates varied significantly with body mass (model II regression; normodense: r_{22}=0.24, P=0.27; max: r_{22}=–0.14, P=0.27). Muscle efficiencies during both normodense and maximal hovering significantly increased with M_b for C_D=1 but were independent of M_b for C_D=3 (Fig. 13). Muscle efficiencies were slightly, but significantly, higher during normodense hovering than during maximal hovering (paired t-test, P=0.0012) for both C_D values.

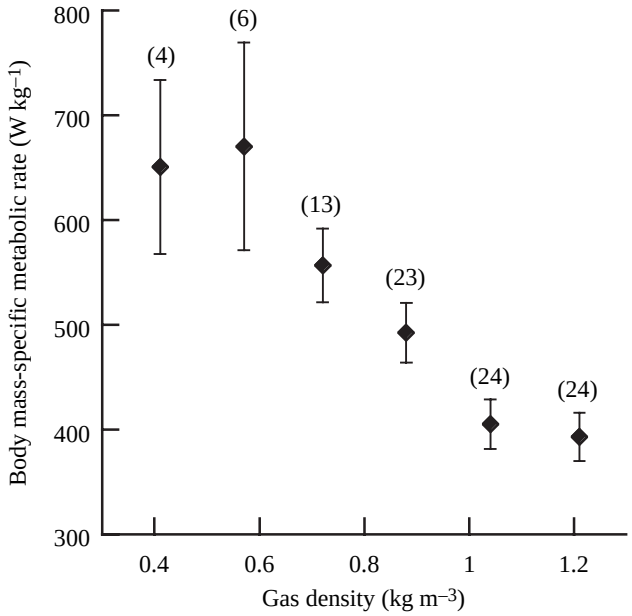

Fig. 11. Body mass-specific metabolic rate during hovering flight (W kg^{-1}) *vs* gas density. Numbers in parentheses indicate the sample sizes at each air density. Error bars represent ± 1 S.E.M.

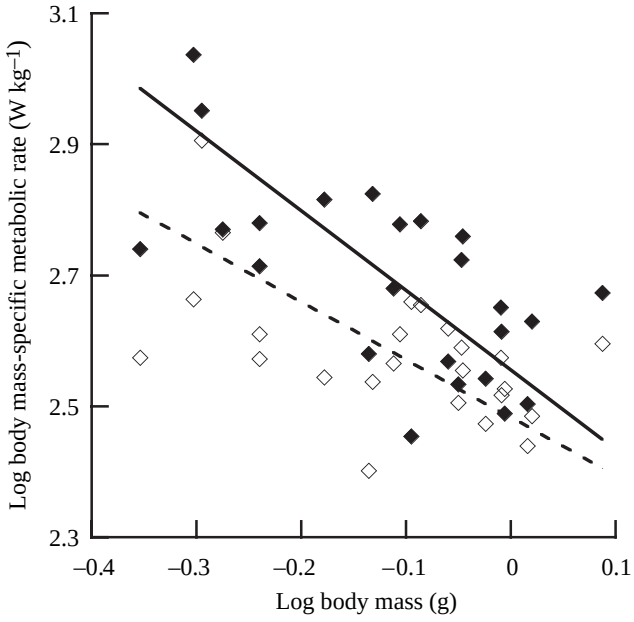

Fig. 12. Log body mass-specific metabolic rate during normal ($P_{met,norm}$; open symbols) and maximal hovering flight ($P_{met,max}$; filled symbols) *vs* log body mass (M_b) for *Xylocopa varipuncta* females. Model II regression: log $P_{met,norm}$=2.483–0.883(log M_b), r_{22}=–0.53, P<0.02 (broken line); log $P_{met,max}$=2.556–1.216(log M_b), r_{22}=–0.64, P<0.001 (solid line).

Thoracic temperatures immediately following flight trials averaged 40.8±1.7°C (mean ± S.D., N=29) and were independent of both M_b (model II regression, r_{27}=0.35, P=0.06) and final gas density (model II regression, r_{27}=0.17, P=0.37).

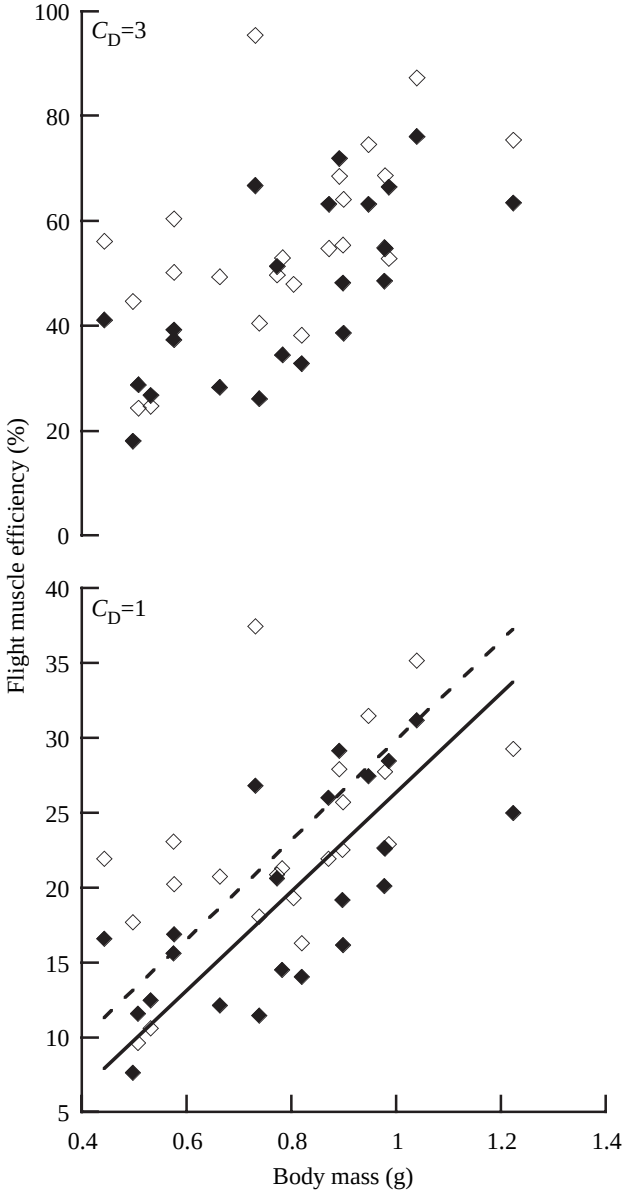

Fig. 13. Flight muscle efficiency during normal (η_{norm}; open symbol) and maximal hovering flight (η_{max}; filled symbols) *vs* body mass (M_b) for *Xylocopa varipuncta* females. Assumed drag coefficient (C_D)=1 (bottom panel) and 3 (top panel). Model II regression for C_D=1: η_{norm}=–3.44+33.28M_b, r_{21}=0.59, P<0.005 (broken line); η_{max}=–6.76+33.12M_b, r_{20}=0.70, P<0.001 (solid line). Model II regression for C_D=3: η_{norm}=–48.34+123.23M_b, r_{21}=0.28, P=0.20; η_{max}=–53.73+117.15M_b, r_{20}=0.39, P=0.07.

Discussion

Using variable-density gas mixtures, we were able to estimate the morphological, kinematic and energetic correlates of maximal hovering flight performance in an insect. For most of the bees in the study, *MGD*s were of densities greater than that of pure heliox (Fig. 2). This finding contrasts with a comparable study of euglossine bees (Dudley, 1995) in which all three species tested were able to fly in pure heliox. It seems

likely that the relatively poor ability of carpenter bees to fly in hypodense gases relates to their higher wing loading: 33 N m^{-2} in *X. varipuncta vs* 21–28 N m^{-2} in the three euglossine species tested by Dudley (1995). In fact, the mean wing loading of the four *X. varipuncta* individuals in this study that were able to fly in pure heliox was at the low end of the range for the species, namely 21.5 N m^{-2}.

Body mass varied nearly threefold among the *X. varipuncta* females used in this study, and the bees were not isometric across this range. Abdomen mass scaled to body mass with a coefficient of 1.69, meaning that the largest bees possessed abdomens that composed nearly 50% of total body mass and were nearly five times heavier than the abdomens of the smallest bees, which represented only 25% of their total body mass. Because the bees were caught in the field, variation in abdominal mass could be partly due to varying nectar loads or reproductive condition, with larger females carrying greater masses of reproductive tissues and eggs. However, nectar loading and reproductive condition could not have been the sole determinants of body mass variation because wing area and thorax mass (parameters that should be unaffected by nectar loading or reproductive status) were 25% and 65%, respectively, higher in the heaviest bees than in the lightest bees. Thorax mass scaled to body mass with a coefficient of 0.63 and, as a consequence, flight muscle composed nearly 50% of the total mass of the smallest bees yet only 25% of the total mass of the largest bees (Fig. 1). Wing loading scaled with body mass with a surprisingly high coefficient of 0.79, compared with a coefficient of 0.33 predicted by isometry and a coefficient of 0.29 based on an empirical multi-species analysis of insects (Dudley, 2000).

Morphological variation had pronounced effects on several performance parameters of hovering flight in *X. varipuncta*. The positive relationship between wingbeat frequency and body mass is unusual given that larger wings have greater inertia and empirical studies of wingbeat frequency almost always show a negative relationship between frequency and body mass (see Dudley, 2000). However, our finding is not unprecedented in that Wekesa et al. (1998) showed that wingbeat frequency is positively correlated with wing length in two species of *Anopheles* mosquitoes. The largest *X. varipuncta*, which had relatively the smallest wings and flight muscles, operated at greater wingbeat frequencies (Fig. 3) and stroke amplitudes (Fig. 4) and lower stroke plane angles (Fig. 6) in normodense hovering than did smaller bees. However, these parameters were independent of body mass during hovering flight at *MGD*. Therefore, the kinematic performance of large bees in normodense hovering approached their limits, whereas smaller bees possessed greater reserve capacities (Fig. 5). Due to their small kinematic reserve capacities, the larger bees experienced aerodynamic failure at higher absolute air densities, with some individuals having *MGD*s only 14% lower than in normal air. Because the major factor driving the decrease in reserve capacity in larger bees was mass allocation to the abdomen, it is possible that *X. varipuncta* suffer a decrease in flight capacity as a cost of increased reproductive ability, as has been shown for dragonflies (Marden, 1989). Such tradeoffs may generally limit the ovarian size of bees and other insects of a given thorax size.

Carpenter bees respond to hypodense aerodynamic challenge by increasing stroke amplitude, as do euglossine bees (Dudley, 1995) and hummingbirds (Chai and Dudley, 1995, 1996). Hovering flight in hypodense gas also elicits small, but significant, increases in wingbeat frequency in carpenter bees and hummingbirds (Chai and Dudley, 1995, 1996) but not in euglossines. Interestingly, carpenter bees and some smaller euglossines (*Euglossa* spp.) decrease stroke plane angle while hovering in hypodense gas, while stroke plane angle is independent of gas density in hummingbirds (Chai and Dudley, 1996) and a larger euglossine, *Eulaema meriana* (Dudley, 1995). *Xylocopa*, like many insect species (Ellington, 1984c; Ennos, 1989; Dudley, 1995) hovers in normodense air at a slightly inclined stroke plane angle. During flight in hypodense gas, the additional 'weight' of the abdomen causes a negative rotation in pitch and perhaps a slight bending at the petiole such that the stroke plane angle approaches true horizontal and the body angle becomes larger. We suspect that similar, although much more subtle, effects occur as a result of proportionately heavier abdomens in larger individuals. Although increasing stroke amplitude was the primary means by which *X. varipuncta* generated additional power during hovering in hypodense gas, smaller bees were also aided by the modest increase in wingbeat frequency because the profile component of power output increases with the cube of wingbeat frequency. Given the significant increase in mean lift coefficient during hypodense hovering (Fig. 10), it is also highly probable that carpenter bees are employing other lift-generating mechanisms during hypodense hovering such as changing the angle of attack or rotational timing at the transition to each subsequent half-stroke. Further analysis of the kinematic mechanisms used by carpenter bees to generate high lift requires greater temporal resolution of wing motions than that used here.

Limits to hovering flight performance in carpenter bees are indicated by a maximum stroke amplitude of ~140° at the point of hypodense failure (Fig. 4). This value is remarkably constant in spite of the considerable size-mediated variation seen in stroke amplitude during hovering under normodense conditions (see Fig. 4). Maximum stroke amplitudes are similar for euglossines (Dudley, 1995) yet are much higher (~180°) in hummingbirds (Chai and Dudley, 1995), although dramatically different phylogenetic associations preclude direct comparison of wingbeat kinematics between these taxa. Nonetheless, the size-independent constancy of limits to wing motions in carpenter bees is strongly suggestive of an anatomical constraint to angular wing displacements that is much lower than that observed in hummingbirds.

The apparent constraint on wingbeat kinematics, and thus on aerodynamic force production, may also be congruent with limits to power availability, at least for larger bees. Assumed values of C_D had significant effects on calculated power, with higher power estimates when C_D=3. However, this C_D value

reduced the likelihood of significant allometries for power, reserve capacity and muscle efficiency, despite significant allometries for kinematic variables and their reserve capacities (Figs 7–9). For this reason, and the fact that muscle efficiencies were unrealistically high (50–60%) when C_D=3 (Fig. 13), we believe that the assumption of C_D=1 is more valid for hovering *Xylocopa*. Under this more reasonable C_D value, maximum muscle mass-specific power output increases substantially with increased body size (Fig. 8), reaching ~400 W kg^{-1} flight muscle in the largest individuals. However, the larger bees, with their relatively smaller flight muscle mass, fail in hovering at similar stroke amplitudes (Fig. 4) and body mass-specific power outputs (Fig. 7) reached by smaller bees. Excess capacity in mechanical power output is relatively smaller in larger bees and appears to approach a limit near the upper end of the body size range (Fig. 9). This finding is suggestive of limits on power production in larger bees that may also coincide with constraints on wing motions. Smaller bees, by contrast, have more capacity to increase stroke amplitude (Fig. 5) and, to a lesser degree, power production (Fig. 9) but nonetheless fail at limiting values of the former quantity. In general, excess lift and power capacity under hypodense but normobaric conditions is probably associated with the requirement in normodense air for supplemental power in vertical ascent, climbing flight or for translational accelerations and fast forward flight. The present data nonetheless demonstrate, over a threefold intraspecific range of body masses, a pronounced size dependence of maximum flight performance that is mediated primarily by the relative amount of flight muscle.

Maximum power output observed in carpenter bees lies close to mean values of power output (based on unsteady values of C_D – see Introduction) estimated for ruby-throated hummingbirds (Chai and Dudley, 1995, 1996) that failed to sustain hovering in similar hypodense conditions and also lies within the range for three species of euglossine bees flying in heliox (Dudley, 1995). One of these euglossine species was comparable in body mass to the carpenter bees studied here (*E. meriana*; 820 mg) and exhibited the highest value of the three species for mechanical power output. Maximal flight performance, even in hovering flight, may also be strongly context dependent. For example, ruby-throated hummingbirds engaged in vertical load-lifting exhibit short-duration but high-intensity power outputs that exceed by 50% the maxima found in density-reduction trials (Chai et al., 1997). Similar experiments with carpenter bees that demonstrated stroke amplitudes or mechanical power outputs exceeding those in hypodense air would clearly necessitate re-evaluation of proposed anatomical constraints on flight performance. Hypodense but hyperoxic gas mixtures might also elicit hovering capacities supplemental to those exhibited here (e.g. Harrison and Lighton, 1998).

As with stroke amplitude and mechanical power output, metabolic rates of hovering carpenter bees substantially increased under hypodense challenge (Figs 11, 12). Maximal mass-specific power output increased by an average of 10% and metabolic rate by 33% compared with during normal hovering. These increases in power output relative to normal hovering are somewhat less than the 45% estimated for euglossine bees (Dudley, 1995). The relatively low power and metabolic scope of carpenter bees, particularly larger individuals, may occur because the higher wing loading of these reproductive females requires them to utilize rates of power production close to their maximal capacities just to hover. Indeed, the smallest bees in the present study, with wing loading values more similar to those of the euglossines, had power scopes approaching 20%.

Flight muscle efficiencies of individual bees, by contrast, were only slightly different between normo- and hypodense conditions (Fig. 13), indicating that increases in mechanical power output are matched by comparable increases in metabolic power input. Again, efficiencies averaged 50–60% when C_D was assumed to be 3, indicating that this assumed value is probably less realistic than a value of 1, which yielded efficiencies averaging 20–25%. Muscle efficiencies thus tend to increase systematically with increased body size (assuming C_D=1), approximately doubling across the size range of bees in this study. This trend was also noticed by Casey et al. (1985) in an interspecific comparison of euglossine bees in normodense hovering and has been described for volant taxa in general (Ellington, 1991; Harrison and Roberts, 2000). The increase in efficiency with size has most commonly been attributed to lower cycle frequencies, with consequent savings in muscle efficiencies. However, this cannot explain the size effects on efficiency during maximal power production in this study as bees of different sizes had similar wingbeat frequencies (Fig. 3). During maximal hovering, none of the kinematic variables varied with mass (Figs 3, 4, 6) and neither did body mass-specific power output differ with size (Fig. 7). Flight muscle mass-specific power output significantly increased with size as the larger bees required more power from their relatively small flight muscles to keep them aloft. Efficiency increased because this greater muscle mass-specific power output occurred at similar muscle-specific metabolic rates, with greater power requirements in larger bees perhaps due to higher C_Ds in these individuals.

The mechanisms responsible for the positive correlation between size and efficiency are unclear. There could be differences in the efficiency of conversion of muscular power to wing mechanical power; for example, elastic energy storage within the thorax may increase with size in this species. Finally, there could be size-related differences in the use of lift-generation mechanisms such as leading edge vortices, wake capture and clap-and-fling (see Dudley, 2000; Birch and Dickinson, 2001; Sane and Dickinson, 2001).

Despite the higher muscle efficiencies of larger carpenter bees, reserve capacity for hovering flight declines at larger body sizes. This effect derives from the disproportionate increase in thoracic muscle mass at smaller body sizes. In summary, larger carpenter bees exhibit absolutely greater maximal muscle mass-specific power outputs than smaller bees but are less capable of flying in hypodense air because of the negative intraspecific allometry of flight muscle mass.

List of symbols

AR	wing aspect ratio
C_D	drag coefficient
C_L	lift coefficient
$C_{L,max}$	mean lift coefficient during maximal hovering flight
$C_{L,norm}$	mean lift coefficient during normal hovering flight
f	wingbeat frequency
f_{max}	wingbeat frequency during hovering in hypodense air
f_{norm}	wingbeat frequency during hovering in normodense air
f_{res}	reserve capacity in wingbeat frequency
$\boldsymbol{g}$	gravitational acceleration
M_b	body mass
M_{muscle}	relative thoracic muscle mass
M_w	relative wing mass
$P_{body,max}$	body mass-specific power output during maximal hovering flight
$P_{body,norm}$	body mass-specific power output during normal hovering flight
P_{ind}	induced power requirement
P_{input}	metabolic power input
P_{mech}	total mechanical power output
$P_{met,max}$	body mass-specific metabolic rate during maximal hovering flight
$P_{met,norm}$	body mass-specific metabolic rate during normal hovering flight
$P_{muscle,max}$	muscle mass-specific power output during maximal hovering flight
$P_{muscle,norm}$	muscle mass-specific power output during normal hovering flight
P_{pro}	profile power requirement
P_{res}	reserve capacity in muscle mass-specific power output
p_w	wing loading
R	wing length
S	total wing area
β	stroke plane angle
β_{max}	stroke plane angle during maximal hovering
β_{norm}	stroke plane angle during normal hovering
χ	body angle
Φ	stroke amplitude
Φ_{max}	stroke amplitude during maximal hovering
Φ_{norm}	stroke amplitude during normal hovering
Φ_{res}	reserve capacity in stroke amplitude
η_{max}	flight muscle efficiency during maximal hovering flight
η_{norm}	flight muscle efficiency during normal hovering flight

We thank Michael Dickinson, Dan Thompson and an anonymous reviewer for helpful comments on the manuscript, and the NSF (IBN 9986163 to S.P.R.; IBN 9985857 to J.F.H.; IBN 9817138 to R.D.) for research support.

References

Birch, J. M. and Dickinson, M. H. (2001). Spanwise flow and the attachment of the leading-edge vortex on insect wings. *Nature* **412**, 729-733.

Casey, T. M., May, M. L. and Morgan, K. R. (1985). Flight energetics of euglossine bees in relation to morphology and wing stroke frequency. *J. Exp. Biol.* **116**, 271-289.

Chai, P., Chen, J. S. and Dudley, R. (1977). Transient hovering performance of hummingbirds under conditions of maximal loading. *J. Exp. Biol.* **200**, 921-929.

Chai, P. (1997). Hummingbird hovering energetics during moult of primary flight feathers. *J. Exp. Biol.* **200**, 1527-1536.

Chai, P. and Dudley, R. (1995). Limits to vertebrate locomotor energetics suggested by hummingbirds hovering in heliox. *Nature* **377**, 722-725.

Chai, P. and Dudley, R. (1996). Limits to flight energetics of hummingbirds hovering in hypodense and hypoxic gas mixtures. *J. Exp. Biol.* **199**, 2285-2295.

Chai, P. and Dudley, R. (1999). Maximum flight performance of hummingbirds: capacities, constraints, and trade-offs. *Am. Nat.* **153**, 398-411.

Chai, P., Harrykissoon, R. and Dudley, R. (1996). Hummingbird hovering performance in hyperoxic heliox: effects of body mass and sex. *J. Exp. Biol.* **199**, 2745-2755.

Chappell, M. A. (1982). Temperature regulation of carpenter bees (*Xylocopa californica*) foraging in the Colorado desert of southern California. *Physiol. Zool.* **55**, 267-280.

Dickinson, M. H. and Lighton, J. R. B. (1995). Muscle efficiency and elastic storage in the flight motor of *Drosophila*. *Science* **268**, 87-90.

Dickinson, M. H., Lehmann, F. O. and Sane, S. P. (1999) Wing rotation and the aerodynamic basis of insect flight. *Science* **284**, 1954-1960.

Dudley, R. (1995). Extraordinary flight performance of orchid bees (Apidae, Euglossini) hovering in heliox (80 percent He/20 percent O_2). *J. Exp. Biol.* **198**, 1065-1070.

Dudley, R. (2000). *The Biomechanics of Insect Flight: Form, Function, Evolution*. Princeton, NJ: Princeton University Press.

Dudley, R. and Chai, P. (1996). Animal flight mechanics in physically variable gas mixtures. *J. Exp. Biol.* **199**, 1881-1885.

Ellington, C. P. (1984a). The aerodynamics of hovering insect flight. I. The quasi-steady analysis. *Phil. Trans. R. Soc. Lond. B* **305**, 1-15.

Ellington, C. P. (1984b). The aerodynamics of hovering insect flight. II. Morphological parameters. *Phil. Trans. R. Soc. Lond. B* **305**, 17-40.

Ellington, C. P. (1984c). The aerodynamics of hovering insect flight. III. Kinematics. *Phil. Trans. R. Soc. Lond. B* **305**, 41-78.

Ellington, C. P. (1984d). The aerodynamics of hovering insect flight. IV. Aerodynamic mechanisms. *Phil. Trans. R. Soc. Lond. B* **305**, 79-113.

Ellington, C. P. (1984e). The aerodynamics of hovering insect flight. V. A vortex theory. *Phil. Trans. R. Soc. Lond. B* **305**, 115-144.

Ellington, C. P. (1984f). The aerodynamics of hovering insect flight. VI. Lift and power requirements. *Phil. Trans. R. Soc. Lond. B* **305**, 145-181.

Ellington, C. P. (1991). Limitations on animal flight performance. *J. Exp. Biol.* **160**, 71-91.

Ennos, A. R. (1989). The kinematics and aerodynamics of the free flight of some Diptera. *J. Exp. Biol.* **142**, 49-85.

Gäde, G. and Auerswald, L. (1998). Flight metabolism in carpenter bees and primary structure of their hypertrehalosaemic peptide. *Exp. Biol. Online* (1998) 3:6.

Harrison, J. F., Fewell, J. H., Roberts, S. P. and Hall, H. G. (1996b). Achievement of thermal stability by varying metabolic heat production in flying honeybees. *Science* **274**, 88-90.

Harrison, J. F. and Lighton, J. R. B. (1998). Oxygen-sensitive flight metabolism in the dragonfly *Erythemis simplicicollis*. *J. Exp. Biol.* **201**, 1739-1744.

Harrison, J. F. and Roberts, S. P. (2000). Flight respiration and energetics. *Annu. Rev. Physiol.* **62**, 179-205.

Heinrich, B. (1975). Thermoregulation in bumblebees. II. Energetics of warm-up and free flight. *J. Comp. Phys.* **96**, 155-166.

Heinrich, B. and Buchmann, S. L. (1986). Thermoregulatory physiology of the carpenter bee, *Xylocopa varipuncta*. *J. Comp. Physiol. B* **156**, 557-562.

King, M. J., Buchmann, S. L. and Spangler, H. (1996). Activity of asynchronous flight muscle from two bee families during sonication (buzzing). *J. Exp. Biol.* **199**, 2317-2321.

Lehmann, F. O. (1999). Ambient temperature affects free-flight performance in the fruit fly *Drosophila melanogaster*. *J. Comp. Physiol. B* **169**, 165-171.

Lehmann, F. O. and Dickinson, M. H. (1997). The changes in power requirements and muscle efficiency during elevated force production in the fruit fly *Drosophila melanogaste*r. *J. Exp. Biol*. **200**, 1133-1143.

Lehmann, F. O. and Dickinson, M. H. (1998). The control of wing kinematics and flight forces in fruit flies (*Drosophila* spp.). *J. Exp. Biol.* **201**, 385-401.

Lehmann, F. O., Dickinson, M. H. and Staunton, J. (2000). The scaling of carbon dioxide release and respiratory water loss in flying fruit flies (*Drosophila* spp.). *J. Exp. Biol.* **203**, 1613-1624.

Marden, J. H. (1987). Maximum lift production during takeoff in flying animals. *J. Exp. Biol.* **130**, 235-258.

Marden, J. H. (1989). Bodybuilding dragonflies: costs and benefits of maximizing flight muscle. *Physiol. Zool*. **62**, 505-521.

Nicolson, S. W. and Louw, G. N. (1982). Simultaneous measurement of evaporative water loss, oxygen consumption and thoracic temperature during flight in a carpenter bee. *J. Exp. Zool*. **222**, 287-296.

Raynor, J. M. V. and Thomas, A. L. R. (1991). On the vortex wake of an animal flying in a confined volume. *Phil. Trans. R. Soc. Lond. B* **334**, 107-117.

Reid, R. C., Prausnitz, J. M. and Poling, B. E. (1987). *The Properties and Gases and Liquids*. Fourth edition. New York: McGraw-Hill.

Roberts, S. P., Harrison, J. F. and Hadley, N. F. (1998). Mechanisms of thermal balance in flying *Centris pallida* (Hymenoptera: Anthophoridae). *J. Exp. Biol*. **201**, 2321–2331.

Roberts, S. P. and Harrison, J. F. (1999). Mechanisms of thermal stability during flight in the honeybee *Apis mellifer*a. *J. Exp. Biol.* **202**, 1523-1533.

Sane S. P. and Dickinson, M. H. (2001). The control of flight force by a flapping wing: lift and drag production. *J. Exp. Biol*. **204**, 2607-2626.

Spangler, H. G. and Buchmann, S. L. (1991). Effects of temperature on wingbeat frequency in the solitary bee *Centris caesalpiniae* (Anthophoridae: Hymenoptera). *J. Kansas Entomol. Soc*. **64**, 107-109.

Usherwood, J. R. and Ellington, C. P. (2002). The aerodynamics of revolving wings. II. Propeller force coefficients from mayfly to quail. *J. Exp. Biol.* **205**, 1565-1576.

Wekesa, J. W., Brogdon, W. G., Hawley, W. A. and Besansky, N. J. (1998). Flight tone of field-collected populations of *Anopheles gambiae* and *Anarabiensis* (Diptera: Culicidae). *Physiol. Entomol.* **23**, 289-294.

Willmott, A. P. and Ellington, C. P. (1997). The mechanics of flight in the hawkmoth *Manduca sexta*. 2. Aerodynamic consequences of kinematic and morphological variation. *J. Exp. Biol.* **200**, 2723-2745.

Wolf, T. J., Schmid-Hempel, P., Ellington, C. P. and Stevenson, R. D. (1989). Physiological correlates of foraging efforts in honey-bees: oxygen consumption and nectar load. *Funct. Ecol*. **3**, 417-424.